

Review

Microstructures, Corrosion Resistance and Wear Resistance of High-Entropy Alloys Coatings with Various Compositions Prepared by Laser Cladding: A Review

Kefeng Lu ¹, Jian Zhu ^{1,*}, Delin Guo ¹, Minghui Yang ¹, Huajian Sun ¹, Zekun Wang ¹, Xidong Hui ²
and Yongling Wu ^{1,*} 

¹ School of Mechanical Engineering, Shandong University of Technology, Zibo 255000, China; feng_look@163.com (K.L.); guodelin1@163.com (D.G.); ymh15615635525@163.com (M.Y.); sun15376687391@163.com (H.S.); wzk1178621805@163.com (Z.W.)

² State Key Laboratory for Advanced Metals and Materials, University of Science and Technology Beijing, Beijing 100083, China; xdhui@ustb.edu.cn

* Correspondence: zhujian@sdut.edu.cn (J.Z.); ylwu06@sdut.edu.cn (Y.W.)

Abstract: Nowadays, high-entropy alloys (HEAs) have become a hot research topic in the field of coating materials. However, HEAs have a large wide range of compositional systems, and the differences in their composition inevitably lead to the significant variations in the matching process parameters of laser cladding and post-treatment methods, which in turn give the coatings a broad range of microstructures and protective properties. Therefore, it is crucial to review and summarize the research progresses on laser cladding HEA coatings to provide a reference for obtaining high-performance HEA coatings and further expand the application of HEA coatings. This work describes the working mechanism of laser cladding and illustrates the advantages and drawbacks of laser cladding in detail. The effects of the addition of alloying elements, process parameters and post-treatment techniques on the microstructures and properties of the coatings are thoroughly reviewed and analyzed. In addition, the correlations between the chemical compositions of HEAs, process parameters of laser cladding, post-treatment techniques and the microstructure and protective properties of the coatings are investigated and summarized. On this basis, the future development direction of HEA coatings is outlined.

Keywords: high entropy alloy coating; preparation process; research progress; microstructure; performance



Citation: Lu, K.; Zhu, J.; Guo, D.; Yang, M.; Sun, H.; Wang, Z.; Hui, X.; Wu, Y. Microstructures, Corrosion Resistance and Wear Resistance of High-Entropy Alloys Coatings with Various Compositions Prepared by Laser Cladding: A Review. *Coatings* **2022**, *12*, 1023. <https://doi.org/10.3390/coatings12071023>

Academic Editors: Hideyuki Murakami and Claudio Mele

Received: 7 June 2022

Accepted: 15 July 2022

Published: 19 July 2022

Publisher's Note: MDPI stays neutral with regard to jurisdictional claims in published maps and institutional affiliations.



Copyright: © 2022 by the authors. Licensee MDPI, Basel, Switzerland. This article is an open access article distributed under the terms and conditions of the Creative Commons Attribution (CC BY) license (<https://creativecommons.org/licenses/by/4.0/>).

1. Introduction

In 2004, Professor B. Cantor of Cambridge University and Professor J. W. Yeh of Tsinghua University in Taiwan reported a new approach for multiple principal component alloy design and opened up the development route of high entropy alloys (HEAs) with multiple principal elements [1,2]. HEAs generally have five or more components, and the atomic fraction of each component ranges from 5 to 35%. After solidification, HEAs do not represent a large number of intermetallic compounds but take their shape in a structure dominated by simple BCC, FCC, or HCP solid solutions [3–6]. The subversive design strategy of HEAs has greatly broadened the field of alloy design and aroused considerable attention from scholars, scientific research institutions, and business circles. The mixing entropy effect of HEAs is different from that of traditional alloys, such as having high a entropy effect, hysteresis diffusion, lattice distortion and “cocktail” effect [7–9]. In addition, the random distribution of multi-component solid solution elements and the addition of easily passivated elements, wear-resistant elements, and oxidation-resistant elements render it better than the traditional metal coating materials in terms of corrosion resistance [10–14], wear resistance [15–18], and oxidation resistance [19–21].

Due to the element content of HEA being much higher than that of traditional engineering alloys, block HEAs have not been applied on a large scale in the industrial field

due to cost constraints. As a coating material, HEAs not only offer advantages of excellent corrosion resistance [22–24], wear resistance [25,26], and oxidation resistance [27], but also overcome the disadvantages of high engineering application costs, which is the primary direction of the development of HEAs. In addition, HEAs have certain requirements for the cooling speed and undercooling degree in the preparation process, and the coating has the characteristics of fast cooling due to the small forming scale, which can effectively inhibit the generation of intermetallic compounds during the forming [28–32]. At present, the main methods of preparing HEAs coatings is laser cladding [33–35].

So far, most of the researches on the preparation process of HEAs coating are focused on the optimization of process parameters, and there is no summary of the correlations between process parameters, microstructure and properties. Meanwhile, the induction of composition regulation and heat treatment modification of HEA coatings are still insufficient. In this review, we attempt to summarize the recent research progress on HEA coatings, introduce the working principle of each preparation process in detail, and focus on the influences of composition control, process parameters, and heat treatment methods on the microstructure and properties of the coatings, in order to obtain high-performance HEA coatings and provide a reference base for broadening the applications of HEA coatings. In addition, the correlations between the chemical compositions of HEAs, process parameters of laser cladding, post-treatment techniques and the microstructure and protective properties of the coatings were investigated and summarized. On this basis, the future development direction of HEA coatings are prospected.

2. Laser Cladding HEAs Coatings

Nowadays, there are many techniques to prepare HEA coatings, which can be classified into hot forming processes and cold forming processes according to the working temperature. Generally, the typical hot forming process are laser cladding and thermal spraying while the common cold forming techniques are electric spark deposition and magnetron sputtering. The coating prepared by cold forming techniques has high a forming quality, high bonding strength, and a uniform coating structure, but it has strict requirements for working conditions (needs a vacuum system), cannot be realized on-site, and the thickness of the prepared coating is limited to a certain extent. For hot forming techniques, prefabricated HEA powder is heated and melted on the substrate and then cooled quickly to form the coating. Laser cladding is used to melt the cladding powder material by laser heating to form the cladding layer. This kind of process is simple to operate and can use on-site preparation, but it has high requirements for powder particle size, and a large amount of protective gas is required in the preparation process to prevent particles from being heated and oxidized.

Due to its high energy density and fast solidification rate, laser cladding technology can avoid element segregation and improve the solubility limit; the prepared coating has a fine structure, superior bonding strength with the substrate, low dilution, and a small heat-affected zone. Therefore, it is particularly suitable for the preparation of HEA coatings. Its working principle is illustrated in Figure 1. Laser cladding uses a high-power density laser beam to heat and melt the surface of the material with no contact, and then rapidly cools of the cladding material to form cladding layers with different properties and microstructures to realize surface modification. Element types, process parameters, heat treatment, and ultrasonic assistance play an essential role to ensure quality of the coating.

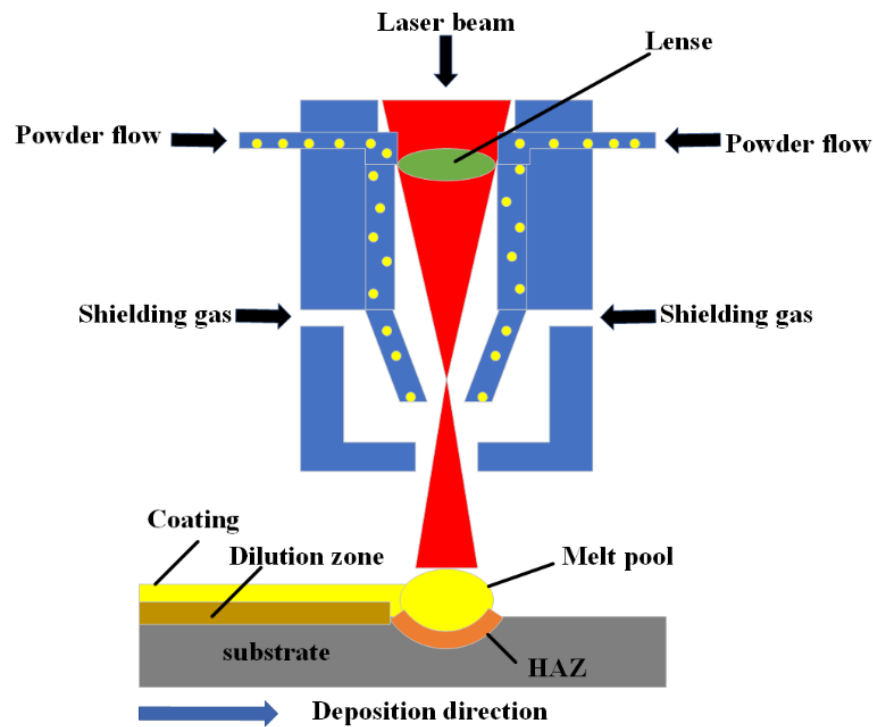


Figure 1. Schematic representation of laser cladding technology.

2.1. The Chemical Composition System of Laser Cladding HEA Coatings

HEA obtains the required properties by adding a group of secondary alloying elements based on one or two main elements. Different types and contents of elements have different effects on the properties of HEA coatings prepared by laser cladding technology. Prior research showed that the proper addition of Si and other self-fusible non-metallic elements has a great impact on the microstructure and properties of HEA coatings. These elements usually have strong slagging and deoxidation abilities, which is conducive to improving the wear resistance and processability of the coating. Bingqian Wu et al. [36] studied the effect of Si content on the microstructure and wear resistance of $\text{FeCoCr}_{0.5}\text{NbSi}_{0.4}$ HEA coatings; the results showed that with the increase of Si content, the microstructure of the coating changed obviously, the M_2B phase decreased, the eutectic structure also disappeared gradually, and the wear resistance of the coating at $\text{FeCoCr}_{0.5}\text{NbSi}_{0.4}$ was the best. During wear, the phases with low hardness values are fatigued off by the cyclic action of the WC balls, while the phases with higher hardness are not worn off, which shows that the wear mechanism of the $\text{FeCoCr}_{0.5}\text{NiBSi}_{0.4}$ high-entropy alloy coating is mainly fatigue wear. Wenjun Hao et al. [37] did similar research, and the results showed that the appropriate addition of Si can reduce the melting point of the alloy and improve the wetting ability. Si also plays a role in grain refinement and improves the hardness and wear resistance of the alloy. The main form of wear on the surface of CoCrFeNi high-entropy alloy coatings is adhesive wear; with the increase of Si content, the main wear mode changes to abrasive wear. CoCrFeNiMo HEA contains many corrosion-resistant elements, such as Cr, Ni, and Mo; the addition of Cr and Ni can form a dense oxide film to resist corrosion, and the addition of Mo can effectively prevent pitting corrosion. In addition, Mo can form a hard Mo-rich phase or Mo atoms can be dissolved into the FCC matrix, so as to obtain higher hardness and wear-resistance coatings and improve the overall properties of the alloy. Fu Yu et al. [38] studied the microstructure, hardness, wear, corrosion, and friction corrosion of laser cladding $\text{CoCr}_2\text{FeNiMo}_x$ ($x = 0, 0.1, 0.2, 0.3, 0.4$) coatings; the results showed that the addition of Mo significantly improved the hardness and wear resistance of the alloy. It can be seen from Figure 2 that the appropriate addition of Mo can promote the formation of the passive film, delay the enlargement of corrosion pit on the alloy

surface and improve the corrosion resistance of the alloy. The friction and corrosion of the Mo-containing coating is due to the combined effects of adhesive wear and corrosion. Biao Huang et al. [39] studied the effect of Cr on the microstructure and properties of HEA coatings. CoFeNiB HEA coating is composed of an FCC solid solution + M_2B phase eutectic structure and an M_2B phase; with the addition of Cr, the M_2B phase decreases, the morphology of the eutectic structure changes from a honeycomb to lamellar structure, and the hardness decreases gradually. Adding elements with a large atomic radius can effectively enhance the lattice distortion effect of HEA, but the effect of element content on the properties of the alloy needs to be further explored. The addition of Al can promote the formation of the BCC phase, to enhance the hardness and high-temperature oxidation resistance of the alloy. Qing-Long Xu et al. [40] investigated the effect of Al content on the high-temperature oxidation resistance of $CuAl_xNiCrFe$ HEAs, and found that with the increase of Al content, the structure of the $CuAl_xNiCrFe$ bonding layer changed from columnar crystal to equiaxed crystal. After 100 h of oxidation at 1100 °C, the $CuAl_xNiCrFe$ coating showed a very low Al diffusion coefficient. It can be observed in Figure 3 that the grain size of $CuAl_xNiCrFe$ increases by only about 20%. The structure and properties of HEA can be modified by doping rare earth elements or carbides. Xulong An et al. [41] studied the effect of WC particles on the microstructure and properties of laser cladding HEA $SiFeCoCrTi$ coatings, and found that after adding WC, the microstructure of the coating changed from cellular dendrite to dense and fine dendrite, and the hardness of the coating increased, the friction coefficient decreased and the wear resistance improved. Alloy surface wear is a combination of abrasive wear and oxidation wear, and the wear surface is rough. Adding ceramic reinforced particles is another strengthening method of HEA coatings. Ceramic particles can effectively limit the grain growth and limit the plastic deformation of the HEA matrix as a strengthening phase. In addition, during the wear process, raised ceramic particles reduce the contact area between the HEA matrix and friction pair. Therefore, the wear resistance is greatly improved, while the interface between the HEA matrix and the directly added ceramic particles is poor, whereas the ceramic phase synthesized in situ has a better interface adhesion with the HEA matrix. Guanghua Yan et al. [42] successfully prepared in-situ HEA coatings with a functional gradient double-layer structure on the surface of H13 steel by laser cladding technology, which significantly improved the wear resistance of the substrate.

Laser cladding can improve the surface properties of the material without changing the shape and inherent properties of the substrate material, and even repairs the damaged surface. The cladding layer can have a strong metallurgical bonding with the substrate surface with a very shallow heat-affected zone on the substrate. This surface modification technology has the advantages of environmental protection, simplicity, flexibility, being time-saving, and saving materials. Therefore, the research on laser cladding HEA coating has increased rapidly in recent years. A lot of research work has been done on the microstructure, mechanical properties, wear resistance, and corrosion resistance of HEA coatings with different components.

Adding some self-fusible non-metallic elements and elements with a large radius have a significant impact on the microstructure and properties of HEA coatings. In addition, doping rare earth elements or ceramic particles also plays a certain role in improving the properties of HEA coatings. Different types of elements or altered contents of the same element have different effects on HEA coatings. Therefore, to achieve higher quality HEA coatings, we should further explore the influence of elements on the coating properties and find out the optimal element combination and content.

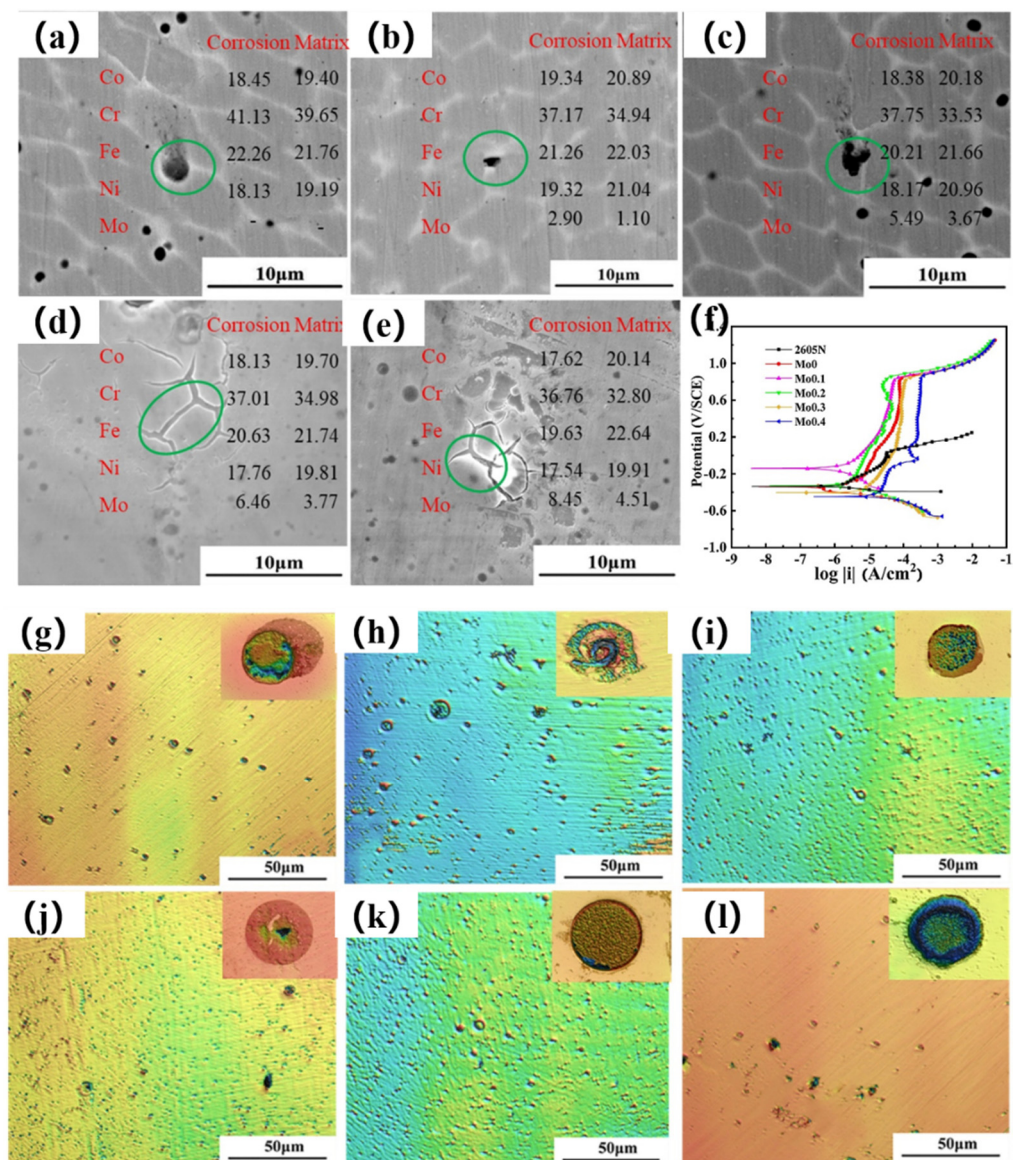


Figure 2. The local corrosion morphology of $\text{CoCr}_2\text{FeNiMo}_x$ ($x = 0, 0.1, 0.2, 0.3, 0.4$) HEA coatings after immersion in 10 wt.% FeCl_3 solution for 10 days, (a) Mo_0 , (b) $\text{Mo}_{0.1}$, (c) $\text{Mo}_{0.2}$, (d) $\text{Mo}_{0.3}$, (e) $\text{Mo}_{0.4}$ (the typical corrosion morphologies are highlighted in the green circles). The compositions of the corrosion region and matrix of the coatings are inserted in the corresponding images. (f) Potentiodynamic polarization curves of coatings on 2605 N stainless steel in 3.5% NaCl solution ($\text{pH} = 2$). Corrosion morphology and pitting morphology of coatings on 2605 N stainless steel at 3.0 °C (g) 2605 N stainless (h) Mo_0 coating (i) $\text{Mo}_{0.1}$ coating (j) $\text{Mo}_{0.2}$ coating (k) $\text{Mo}_{0.3}$ coating (l) $\text{Mo}_{0.4}$ coating (Reprinted with permission from ref. [38]. Copyright 2021 Elsevier).

2.2. The Process Parameters for the Preparation of Laser Cladding HEAs Coatings

In an engineering phenomenon, the accurate control of process parameters is a necessary condition for obtaining a high performance. Similarly, different laser processing parameters in laser cladding technology will affect the characteristics of the cladding layer. The main parameters influencing the performance of the cladding layer include laser power, laser spot size, scanning speed, and powder feeding speed. In addition, the laser beam wavelength, beam profile, defocus distance, and polarization also affect the quality of the cladding layer.

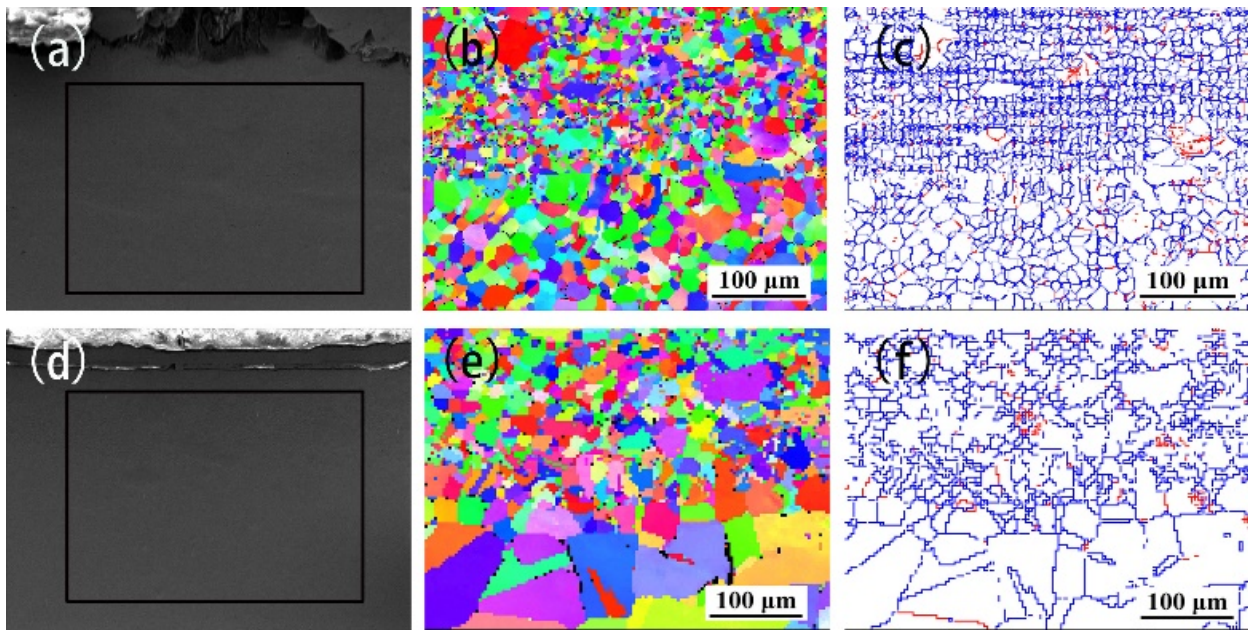


Figure 3. Grain orientation and grain boundaries obtained from EBSD analysis of a cross-section of CuAl_xNiCrFe HEA coatings and a nickel-based superalloy substrate before and after 100 h of oxidation at 1100 °C. (a–c) CuAl_xNiCrFe HEA coatings, (d–f) Nickel-based superalloy substrate (Reprinted with permission from ref. [40]. Copyright 2021 Elsevier).

Different laser process parameters will affect the crack, surface roughness, dilution ratio, and surface macro morphology of HEA coatings. It is reported that if the laser power is too low, the coating will contain unfused powder and pores. If the laser power is too high, the coating will produce microcracks, and the dilution rate will increase, resulting in the weakening of the strengthening effect of the coating on the substrate. Therefore, the generation of defects in the cladding layer can be reduced only under appropriate laser power. The laser beam scanning speed also plays a vital role in forming the quality of the cladding layer. If the scanning speed is too high, it will lead to the incomplete melting of the powder and matrix. If the scanning speed is too low, it will lead to the overheating of the laser cladding layer. Therefore, the analysis and adjustment of the laser beam scanning speed is vitally important to ensure the coating quality. Haijiang Wang et al. [43] studied the effects of the laser power, scanning speed, and diamond content on the microstructure and wear resistance of FeCoCrNi–Mo composite coatings. It was found that the laser cladding process parameters have a significant impact on the dilution ratio, graphitization, and wear resistance of the composite coating. As the laser power decreases, the wear area increases and the plough marks on the wear surface of Si₃N₄ balls increase. When the laser power was 3000 W, the wear area and the number of plough teeth increased sharply, and the wear mechanism changed from adhesive wear to abrasive wear with the best wear resistance of the coating. When the laser power was 3000 W and the scanning speed is 50 mm/s, the composite coating had a uniform microstructure, the lowest dilution ratio, and the best wear resistance. It exhibited a mixed wear mechanism of adhesive wear and abrasive wear. Yaxiong Guo et al. [44] studied the effects of laser power and scanning speed on the surface morphology, hardness, and wear resistance of MoFeCrTiWAlNb HEA coatings. Figure 4 shows the SEM diagram of the cross-section morphology of the coatings with different scanning rate ranges. It can be seen that the coating, fabricated at a scanning rate of 3 mm/s, possesses irregular cellular dendrites and granular carbide particles. With the scanning rate increasing, the dendrites become more regular and uniform in size. When compared with those coatings fabricated at various scanning rates, the HEA coating ($p = 3.0$ kW and $v = 4$ mm/s) exhibited a more homogeneous and denser microstructure with no obvious microcracks. It shows that slow scanning speeds reduced the content of

W-rich particles and restrained the crack initiation while large scanning rates exhibited large numbers of cracks and W-rich particles because of the relatively lower laser energy. Cong Ni et al. [45] studied the effect of laser beam scanning speed on $\text{Al}_{0.5}\text{FeCu}_{0.7}\text{NiCoCr}$ HEA coatings. It was found that when the laser power was 1100 W and the scanning speed was 630 mm/min, the adhesion between the coating and the substrate was the highest, and a defect-free coating with ultra-fine structure was obtained. Fengyuan Shu et al. [46] prepared CoCrBFeNiSi HEA coatings with different levels of laser power. It was found that the coating can be divided into three layers: the bottom dendrite layer, upper amorphous layer, and transition layer. The laser power affects the dilution rate and actual cooling rate of the coating by changing the heat input, to affect the amorphous content in the coating. With the increase of laser power, the amorphous content gradually decreases and the microhardness of the coating decreases. With the increase of laser power, the deeper the groove of the coating, the more serious the adhesive wear and oxidation wear, the larger the cross-sectional area of the wear track, the higher the wear weight loss rate, and the worse the wear resistance of the coating is.

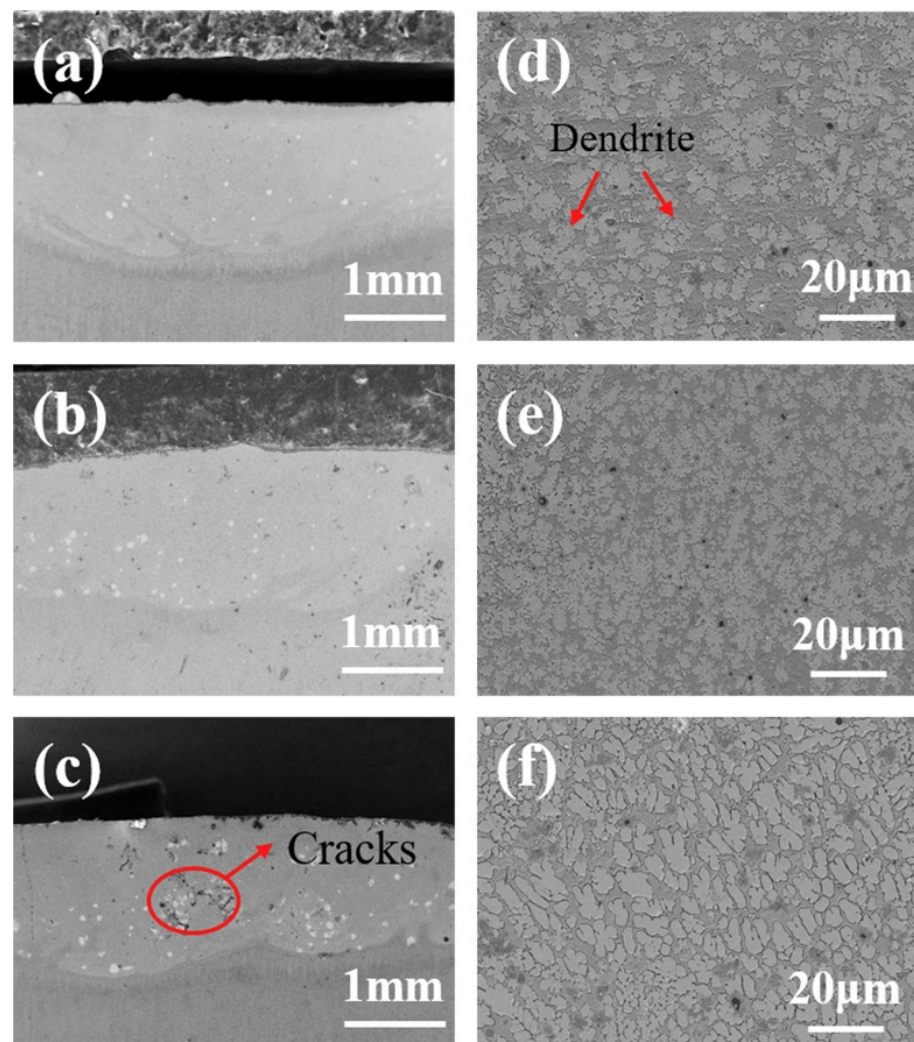


Figure 4. SEM images: (a–c) entire morphology of HEA coatings fabricated by laser cladding with laser power of 3 kW and scanning rate ranging from 3 to 5 mm/s; (d–f) microstructure of middle regions in HEA coatings fabricated by laser cladding with laser power of 3 kW and scanning rate ranging from 3 to 5 mm/s. (Reprinted with permission from ref. [44]. Copyright 2018 Elsevier).

The quality of laser cladding HEA coating is not just affected by laser power and scanning speed; other parameters are also critical to obtain good quality HEA coatings.

Qi Chao et al. [47] studied the effect of powder feeding rate on Al_xCoCrFeNi HEA coatings, and the results demonstrated that the thickness of the cladding layer decreased with the increase of the powder feeding rate. In addition, the height, width, depth, and interdiffusion thickness of the cladding layer increased with the increase of laser power. Xiao Zhao et al. [48] studied the combination of scanning speed, laser power, and powder feeding rate in the process of laser cladding, and obtained the optimal parameter combination.

Different process parameters will affect the surface morphology, microstructure, mechanical properties, wear resistance, and corrosion resistance of laser cladding HEA coatings. When a parameter is improperly selected, the coating will produce defects, including unmelted particles, discontinuous and uneven cladding layer geometry, pores, and microcracks. When the laser power is low or the feeding rate is fast, unmelted particles will appear. When the scanning speed is too fast, discontinuous and uneven cladding geometry, pores and microcracks will be produced. Therefore, to achieve high-quality HEA coatings, various laser processing parameters and their interaction must be considered.

2.3. The Post-Treatment of the Heat Treatment and Ultrasonic Assistance

The microstructure evolution and solid phase transformation of HEA coating during high-temperature heating have a great impact on the material properties. Therefore, it is necessary to study the phase stability and property changes of HEA under different heating temperatures, to provide a clearer basis for the application of HEA on high-temperature applications. Hao Liu et al. [49] studied the effect of heat treatment on the phase stability and wear properties of laser cladding AlCoCrFeNiTi_{0.8} HEA coatings. As can be seen from XRD, SEM, and TEM analyses of the coating in Figure 5, the coating is composed of an FeCr solid solution phase with a BCC lattice and an AlNi precipitate phase with a B2 lattice. It was found that there is no obvious change in the structure below 700 °C; after heat treatment at 900 °C, the coarsening phenomenon of AlNi precipitates could be observed. After heat treatment at 1200 °C, the Ostwald ripening phenomenon of precipitates could be observed. Coarsening of precipitates further leads to the decline of the wear resistance of the material. Due to the high heat generated by laser cladding, the temperature gradient between the substrate and the cladding layer is large, resulting in large residual stress and cracks in the cladding layer. When compared with the substrate material, the cladding material generally has a lower coefficient of thermal expansion. Reducing the temperature gradient between the substrate and the cladding layer by preheating the substrate can effectively avoid cracks. Can Huang et al. [50] studied the dry sliding wear behavior of laser cladding TiVCrAlSi HEA coatings on a Ti-6Al-4V substrate. To avoid cracking, the substrate was preheated at 450 °C. The results showed that there are only a few microcracks and pores in the coating section, and the coating has a good metallurgical bonding ability. The Ti-6Al-4V substrate underwent severe abrasive wear and adhesive wear. The wear surface morphology of the TiVCrAlSi high-entropy alloy coating indicates that the tests occur in a light wear state, with the main material loss mechanisms being oxidation, minor adhesive material transfer, and fragmentation and spalling of the adhesive material (including oxides).

The forming quality of HEA coatings can be improved to a certain extent through certain heat treatments. However, element segregation, inclusion, and structural ripples could be improved with the help of an external field. Ultrasonic cavitation, acoustic flow, and ultrasonic vibration can promote the full mixing, diffusion, and mixing of elements in HEA coatings, therefore, one should significantly avoid stress concentration and homogenize the stress field. The schematic diagram of ultrasonic impact treatment is shown in Figure 6. Meiyang Li et al. [51] studied the effect of ultrasonic shock treatment on the microstructure and properties of laser cladding Al_{0.5}CoCrFeMnNi HEA coatings. The results showed that ultrasonic impact did not change the phase structure of the coating, and there was an obvious solidification boundary in the cladding layer. After one impact, a thin plastic deformation layer was formed. With the increase of impact times, obvious impact marks appeared on the surface. In addition, the original precipitates at the solidification boundary were broken into smaller precipitates, and the particles inside the grain also had cracks.

The minimum surface roughness and maximum surface hardness of the ultrasonic impact layer can be obtained by one impact, and the corrosion resistance of the impact layer was good. Corrosion morphologies showed that typical intergranular corrosion occurred on the surfaces of both kinds of layers while extensive corrosion pits appeared on the cladding coating surfaces. Xin Wen et al. [52] successfully prepared FeCrCoAlMn_{0.5}Mo_{0.1} HEA coatings on the surface of 316 L stainless steel by ultrasonic-assisted laser cladding technology and obtained a coating with no defects, good friction resistance, and corrosion resistance.

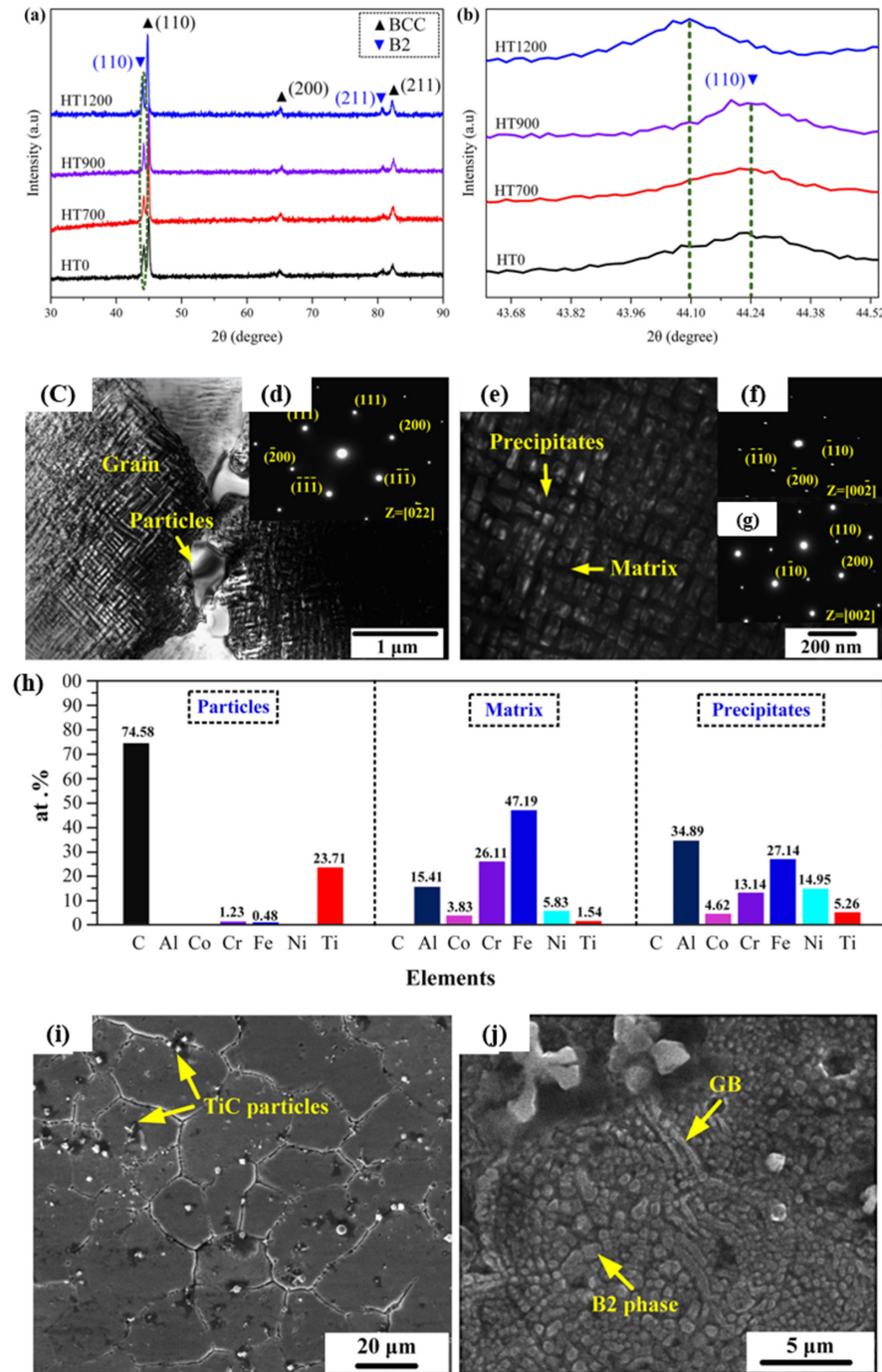


Figure 5. XRD patterns of the HEA coatings: (a) XRD patterns; (b) partial enlarged view; TEM and EDS results of the as-deposited coating: (c) TEM image; (d) SAED pattern of particles; (e) enlarged view of grain; (f) SAED pattern of matrix; (g) SAED pattern of nano-precipitates; (h) EDS results; (i,j) Cross-section SEM images of the HEA coating HT0. (Reprinted with permission from ref. [49]. Copyright 2020 Elsevier).

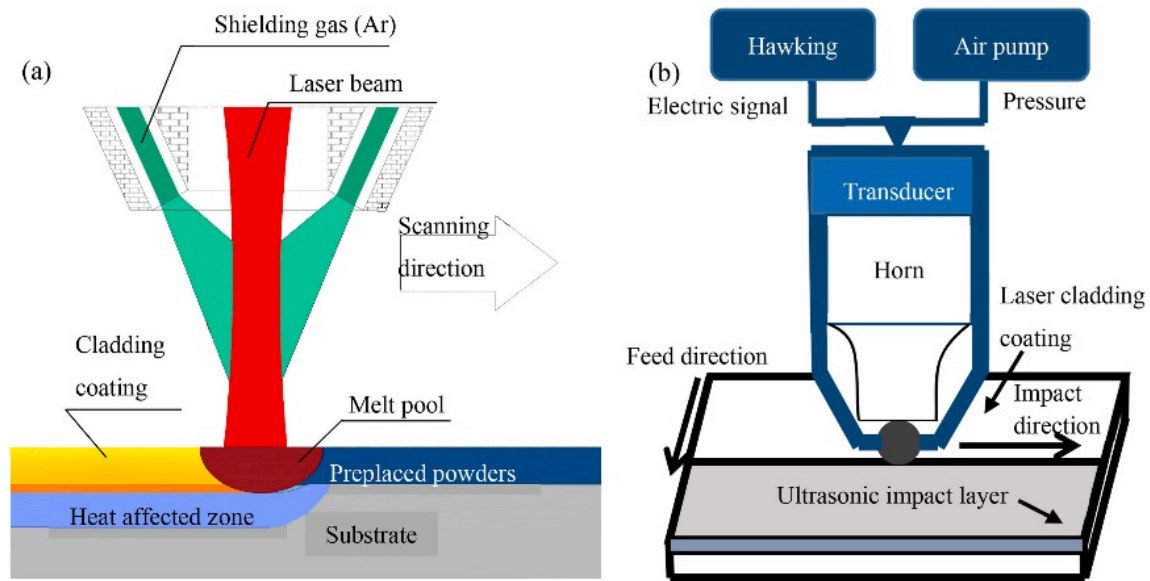


Figure 6. (a) Schematic diagram of laser cladding process; (b) schematic diagram of ultrasonic impact treatment on the surface of laser cladding coatings. (Reprinted with permission from ref. [41]. Copyright 2021 Elsevier).

The residual stress can be effectively eliminated and cracks can be avoided by pre-heat treatment or post-heat treatment of the coating. In addition, preheating the substrate can reduce the temperature gradient between the substrate and the coating, which is conducive to obtaining a defect-free coating. To further improve the surface properties, the subsequent surface treatment methods are very promising. For example, the elements in the HEA coating were fully stirred, diffused, and mixed by ultrasonic assistance, to significantly avoid stress concentration, homogenize the stress field and improve the forming quality of HEA coating.

3. Discussion

Based on the above discussions on the influences of process parameters and HEA compositions on the microstructures and major properties, we summarize the reported data and provide a clear comparison for the laser cladding technology and their achieved properties in Table 1.

Table 1. Overview of process parameters, HEA compositions, microstructures and major properties.

Process Parameters	HEAs	Substrate Materials	Phase (Minor-Major)	All Possible Strengthening Mechanism	Optimal Performance	Ref.
LP 2000 W SR 4 mm/s OR 50%	FeCoCr0.5NiBSix	45 steel	FCC, M ₂ B	Fine grain strengthening	H = 820 HV	[36]
LP 800 W SR 8 mm/s OR 50% SD 2 mm	CoCrFeNiSix	45 steel	FCC at x = 0; FCC + BCC at x = 0.5, 1.0, 1.5, BCC at x = 2.0	Fine grain strengthening	H = 586.5 HV FC = 0.49	[37]
LP 700 W SR 7.5 mm/s OR 40 % SD 1 mm	CoCr2FeNiMox	Q235	FCC at x = 0, 0.1; FCC + σ -CrMo at x = 0.3, 0.4	Solid solution strengthening + precipitation strengthening	H = 724.2 HV FC = 0.42 CP = 29.6 μ A/cm ²	[38]

Table 1. Cont.

Process Parameters	HEAs	Substrate Materials	Phase (Minor-Major)	All Possible Strengthening Mechanism	Optimal Performance	Ref.
LP 1200 W SR 3 mm/s OR 50% SD 2.5 mm	FeCoCr _x NiB	45 steel	FCC + M ₂ B	Solid solution strengthening	H = 860 HV	[39]
LP 2500 W SR 4 mm/s PFR 24 g/min OR 80%	CuAl _x NiCrFe	Nickel-based superalloy	FCC at x = 0.5, 1.0; FCC + BCC at x = 1.5, 2.0	Fine grain strengthening	Excellent oxidation resistance	[40]
LP 3800 W SR 4 mm/s OR 30% SD 3 mm	SiFeCoCrTiWC _x	Q235	BCC + Co _{1.07} Fe _{18.93} at WC = 0; BCC + TiCo ₃ , Co _{1.07} Fe _{18.93} at WC = 0.2	Solid solution strengthening + fine grain strengthening	H = 578.6 HV FC = 0.357 WR = 0.08 mg/min	[41]
LP 3000~5 000 W SR 30~60 mm/min SD 4.6 mm	FeCoCrNi-Mo and diamond	42CrMo steel		Solid solution strengthening	H = 602 HV FC = 0.41	[43]
LP 2400 W~3200 W SR 3~5 mm/s SD 10 × 2 mm	MoFeCrTiWAlNb	M2 tool steel	FCC + (Nb, Ti)C carbides+Fe ₂ Nb		H = 1050 HV FC = 0.55	[44]
LP 1100 W SR 270~630 mm/min SD 2 mm	Al _{0.5} FeCu _{0.7} NiCoCr	5083 aluminum	FCC + BCC		H = 750 HV	[45]
Laser power 233~700 W	CoCrBFeNiSi	H13 steel	FeNi ₃ + β(Co) + Co ₂ B		H = 1192.5 HV FC = 0.14	[46]
LP 3100 W SR 5 mm/s SD 10 × 2 mm	CrFeNiSiAl _{0.5} + chromite powder	40Cr	BCC at chromite powder = 0; BCC + FCC at chromite powder = 10%, 15%	Dispersion strengthening + solid solution strengthening + fine grain strengthening	H = 838.1 HV WR = 0.14 mg/min	[53]
LP 1700 W SR 6 mm/s OR 25% SD 4 mm	FeCoCrNiB _x	Q235	FCC at x = 0.5, 0.75; FCC + M ₃ B at x = 1.0, 1.25	Dispersion strengthening	H = 865.3 HV WR = 0.09 mg/min	[54]
LP 1500 W SR 5 mm/s PFD 3 g/min OR 60% SD 2.5 mm	CoCrFeMnNiTi _x	45 steel	FCC + TiC	Solid solution strengthening + second phase strengthening	H = 364.5 HV FC = 0.72 CP = 4.60 × 10 ⁻⁶ A·cm ⁻²	[55]
LP 3700 W SR 10 mm/s	AlTiVMoNb	TC4	BCC		H = 885.5 HV	[56]
LP 600 W SR 2 mm/s PFD 3.5 g/min SD 1.44 mm	TiZrAlNbCo	TC4	FCC + BCC		H = 689.4 HV CP = 3.66 × 10 ⁻⁹ A/cm ²	[57]

Table 1. Cont.

Process Parameters	HEAs	Substrate Materials	Phase (Minor-Major)	All Possible Strengthening Mechanism	Optimal Performance	Ref.
LP 3600 W SR 3 mm/s OR 50%	CoCrNiTi	Pure Ti sheet	BCC + Laves		H = 762 HV; WR = 1.7×10^{-5} $\text{mm}^3 \cdot \text{N}^{-1} \cdot \text{m}^{-1}$	[58]
LP 3000 W SR 5 mm/s OR 50% SD 6 mm	AlNbTaZrx	Ti ₆ Al ₄ V	BCC + HCP	Fine grain strengthening	H = 650 HV FC = 0.8	[59]
LP 3000 W SR 4 mm/s OR 30% SD 1 mm	CoCrFeNiTi	304	FCC + Laves		CoCrFeNiTi H = 568 HV	[60]

Remarks: Laser power (LP); Scanning rate (SR); Overlap rate (OR); Spot diameter (SD); Hardness (H); Friction coefficient (FC); Wear rate (WR); Corrosion performance (CP).

Most of the studies on HEA coating mainly focus on hardness and wear resistance, Figure 7 shows the hardness and friction coefficient of HEA coating prepared by laser cladding technology. As can be seen from the figure, the hardness of HEA coatings prepared by different processes is mainly concentrated around 500–900 HV, and the friction coefficient is between 0.3 and 0.6.

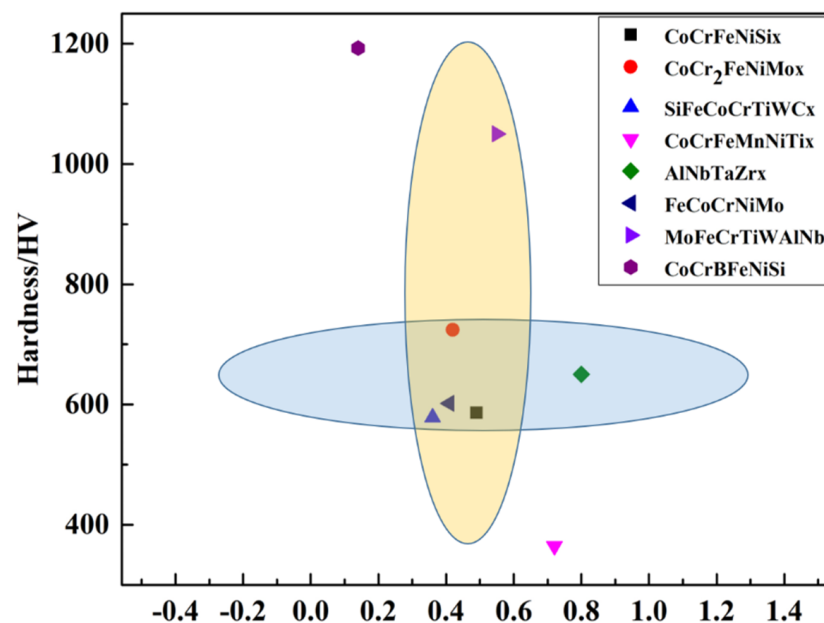


Figure 7. Hardness and friction coefficient of HEA coatings for laser cladding technology.

Laser cladding can avoid element segregation and improve the solubility limit because of its high energy density and fast solidification rate. At the same time, the coating prepared by laser cladding has a fine microstructure, high bonding strength with the substrate, a low dilution rate and a small heat-affected zone. However, because of high heat input, laser cladding easily produces micro-cracks, pores and other defects. In addition, the technology requires a high particle size, and the preparation process requires a large amount of protective gas to prevent the particles from thermal oxidation.

Different kinds and contents of elements have different effects on the properties of HEA coatings. The addition of some self-fluxing non-metallic elements or elements with large radii has a great influence on the microstructure and properties of HEA coatings.

In addition, doping rare earth elements or ceramic particles also plays a certain role in improving the properties of HEA coatings. Different process parameters have a great influence on the properties of HEA coatings, among which laser power, scanning speed and powder feeding rate are the three most important factors affecting the performance of laser cladding HEA coatings. Low laser power will cause the non-melting of powder particles, discontinuous forming of cladding layer, inclusion, non-fusion and other defects. High laser power will lead to high heat input, high heat in the molten pool and increased dilution rate, and the cladding layer is prone to a cracking phenomenon when the laser power is too high. A small scanning speed will lead to high heat input of the molten pool, increased metal melting amount on both sides of the molten pool, larger melting width, larger dilution rate of the cladding layer, as well as a larger size of the cladding layer, which are more likely to cause cracks and other defects. When the scanning speed is larger, the amount of powder feeding and heat input per unit time is reduced, the cladding is high, the melting depth is smaller, the interfacial bonding strength is lower and the strengthening effect on the substrate is weakened. The powder feeding speed is a key factor to determine the thickness of the coating; too high a speed is likely to cause discontinuity in the formation of the coating and a smaller thickness, and too slow a speed will lead to increased heat input per unit of time and the coating being too thick, increasing the tendency of the coating to cracking. Therefore, reasonable selection of each process parameter is the key to obtain high-quality coatings, and the study of the interaction mechanism between each parameter is also of great significance to obtain higher quality HEA coatings. Through the heat treatment of the coating, the residual stress can be effectively eliminated and cracks can be avoided. In addition, the temperature gradient between the substrate and the coating can be reduced by preheating the substrate, which is beneficial to obtain the defect-free coating. In order to further improve the surface properties, the subsequent surface treatment methods are very promising. For example, the elements in the HEA coating are fully stirred, diffused and mixed by ultrasonic assistance, so as to significantly avoid stress concentration, homogenize the stress field and improve the forming quality of the HEA coating.

So far, by optimizing the composition and parameters of HEA coatings prepared by laser cladding, it has been possible to obtain coatings of high quality, but there are still some challenges to be met in bringing HEA to industrial production:

The microstructure and properties of HEA coatings prepared by different processes are very different, and each process has its own advantages and disadvantages. The combination of different processes by studying the working principle of each process has a good prospect to obtain high performance HEA coatings. For example, shot peening on the surface of laser cladding coatings by thermal spraying can effectively improve defects such as microcracks and pores. The kinds and contents of different elements have different effects on the HEA coating. The properties of the coating can be strengthened by adding rare earth elements or ceramic particles, but in order to achieve a higher quality HEA coating, we should further explore the influence of elements on the coating and find out the optimal element combination and content. In addition, the prepared HEA coatings are mainly concentrated in AlCrFeCoNi, AlSiCrFeCoNi, AlTiCrFeCoNi, CrFeCoNi (Mn/Nb/Mo) and other alloy systems, and their applications are mainly concentrated in the fields of corrosion-resistant coatings, wear-resistant coatings, high-temperature oxidation-resistant coatings and so on. In order to broaden the application field of HEA coatings and continue the HEA design concept, it should be a key research direction to continue to develop new spraying materials or to realize the preparation of HEA alloy composite coatings. Process parameters play an important role in obtaining high performance HEA coatings. While studying the influence of various parameters on the forming quality of the coating, we should also explore the synergistic mechanism of the influence of various parameters on the microstructure and properties of the coating. The compound effect of various parameters is reflected by finite element analysis and simulation, so as to provide theoretical reference for the preparation of better HEA coating. Heat treatment can effectively eliminate the residual

stress and microcracks in the coating, but the effect of heat treatment processes on the evolution of the microstructure of the coating is still uncertain, which should be a key research direction. At the same time, the defects such as element segregation, inclusion and structural ripples in the coating can be effectively improved with the help of external field-assisted technology, of which the ultrasonic effect, cavitation effect and vibration effect of ultrasonic-assisted deposition technology can promote the full mixing, diffusion and mixing of various elements in HEA coating, so as to effectively avoid stress concentration, homogenize the stress field and optimize the surface properties of the coating. In addition, reasonable surface treatment methods still need to be further studied.

4. Conclusions and Prospect

In this paper, the status of HEA coatings prepared by laser cladding was reviewed, the relationship between “process method–process parameters–microstructure properties” was summarized. The following main conclusions are drawn.

(1) The main preparation method for HEA coatings is laser cladding. At present, the research on the performance of HEA coatings is mainly focused on corrosion resistance and wear resistance. In order to broaden the application field of HEA coatings, the continuation of the HEA design concept and the development of new coating materials or the preparation of composite coatings of various HEA alloys should be one of the key research directions.

(2) The type and content of HEA elements can have a significant effect on the microstructure and properties of coatings prepared by different processes. To achieve higher quality HEA coatings, the influence of elements on the coatings should be further investigated to find the optimal combination and content of elements.

(3) Different process parameters also have a significant impact on the microstructure and properties of HEA coatings, and the research of process parameter optimization plays an important role in improving the coating quality. The optimization of process parameters plays an important role in improving the coating quality. By studying the working principle of each process, the interplay between different processes is promising for obtaining high performance HEA coatings. The finite element analysis simulations reflect the composite effect of each parameter and provide a theoretical reference for the preparation of better HEA coatings.

(4) Heat treatment of the coating can effectively eliminate residual stresses and avoid the generation of defects such as cracks and porosity, which is conducive to further improving the coating quality. The influence law of heat treatment process on the evolution of the internal microstructure of the coating is still uncertain and should be a key research direction.

Author Contributions: Conceptualization, K.L. and J.Z.; methodology, H.S., D.G. and K.L.; investigation, M.Y., Z.W. and K.L.; writing—original draft preparation, K.L.; writing—review and editing, J.Z. and Y.W.; supervision, X.H. All authors have read and agreed to the published version of the manuscript.

Funding: This work was the financial support of the National Natural Science Foundation of China (52004154), the Shandong Provincial Natural Science Foundation (ZR2020QE002, ZR2020ME047, ZR2020ME164), and the National Key Laboratory Foundation of China (6142005190208).

Institutional Review Board Statement: Not applicable.

Informed Consent Statement: Not applicable.

Data Availability Statement: Data is contained within the manuscript.

Conflicts of Interest: The authors declare no conflict of interest.

References

1. Yeh, J.W.; Chen, S.K.; Lin, S.J.; Gan, J.Y.; Chin, T.S.; Shun, T.T.; Tsau, C.H.; Chang, S.Y. Nanostructured High-Entropy Alloys with Multiple Principal Elements: Novel Alloy Design Concepts and Outcomes. *Adv. Eng. Mater.* **2004**, *6*, 299–303. [[CrossRef](#)]
2. Cantor, B.; Chang, I.T.H.; Knight, P.; Vincent, A.J.B. Microstructural development in equiatomic multicomponent alloys. *Mater. Sci. Eng. A* **2004**, *375*, 213–218. [[CrossRef](#)]
3. Zhang, L.S.; Ma, G.L.; Fu, L.C.; Tian, J.Y. Recent Progress in High-Entropy Alloys. *Adv. Mater. Res.* **2013**, *227*, 631–632. [[CrossRef](#)]
4. Park, T.; Kim, J.H. Tensile properties and microstructure evolution during two-stage tensile testing of CoCrFeMnNi high-entropy alloy. *Mater. Res. Technol.* **2020**, *9*, 7551–7557. [[CrossRef](#)]
5. Liu, F.; Liaw, P.K.; Zhang, Y. Recent Progress with BCC-Structured High-Entropy Alloys. *Metals* **2022**, *12*, 501. [[CrossRef](#)]
6. Xu, X.D.; Guo, S.; Nieh, T.G.; Liu, C.T.; Hirata, A.; Chen, M.W. Effects of mixing enthalpy and cooling rate on phase formation of Al_xCoCrCuFeNi high-entropy alloys. *Materialia* **2019**, *6*, 100292. [[CrossRef](#)]
7. Chang, Y.J.; Yeh, A.C. The evolution of microstructures and high temperature properties of Al_xCo_{1.5}CrFeNi_{1.5}Ti_y high entropy alloys. *J. Alloys Compd.* **2015**, *653*, 379–385. [[CrossRef](#)]
8. Otto, F.; Dlouhý, A.; Somsen, C.; Bei, H.; Eggeler, G.; George, E.P. The influences of temperature and microstructure on the tensile properties of a CoCrFeMnNi high-entropy alloy. *Acta Mater.* **2013**, *61*, 5743–5755. [[CrossRef](#)]
9. Munitz, A.; Kaufman, M.; Nahmany, M.; Derimow, N.; Abbaschian, R. Microstructure and mechanical properties of heat-treated Al₁.25CoCrCuFeNi high entropy alloys. *Mater. Sci. Eng. A* **2018**, *714*, 146–159. [[CrossRef](#)]
10. Wang, Z.; Wu, Q.; Zhou, W.; He, F.; Yu, C.; Lin, D.; Wang, J.; Liu, C.T. Quantitative determination of the lattice constant in high entropy alloys. *Scr. Mater.* **2019**, *162*, 468–471. [[CrossRef](#)]
11. Gludovatz, B.; Hohenwarter, A.; Catoor, D.; Chang, E.H.; George, E.P.; Ritchie, R.O. A fracture-resistant high-entropy alloy for cryogenic applications. *Science* **2014**, *345*, 1153–1158. [[CrossRef](#)]
12. Chuang, M.H.; Tsai, M.H.; Wang, W.R.; Lin, S.J.; Yeh, J.W. Microstructure and wear behavior of Al_xCo_{1.5}CrFeNi_{1.5}Ti_y high-entropy alloys. *Acta Mater.* **2011**, *59*, 6308–6317. [[CrossRef](#)]
13. Chen, J.; Niu, P.; Liu, Y.; Lu, Y.; Wang, X.; Peng, Y.; Liu, J. Effect of Zr content on microstructure and mechanical properties of AlCoCrFeNi high entropy alloy. *Mater. Des.* **2016**, *94*, 39–44. [[CrossRef](#)]
14. Zhang, W.; Liaw, P.K.; Zhang, Y. Science and technology in high-entropy alloys. *Sci. China Mater.* **2018**, *61*, 2–22. [[CrossRef](#)]
15. Daoud, H.M.; Manzoni, A.M.; Wanderka, N.; Glatzel, U. High-Temperature Tensile Strength of Al₁₀Co₂₅Cr₈Fe₁₅Ni₃₆Ti₆ Compositionally Complex Alloy (High-Entropy Alloy). *JOM* **2015**, *67*, 2271–2277. [[CrossRef](#)]
16. He, J.Y.; Liu, W.H.; Wang, Y.; Wu, Z.; Lu, P. Effects of Al addition on structural evolution and tensile properties of the FeCoNiCrMn high-entropy alloy system. *Acta Mater.* **2014**, *62*, 105–113. [[CrossRef](#)]
17. Fu, Z.; Yang, B.; Gan, K.; Yan, D.; Li, Z.; Gou, G.; Chen, H.; Wang, Z. Improving the hydrogen embrittlement resistance of a selective laser melted high-entropy alloy via modifying the cellular structures. *Corros. Sci.* **2021**, *190*, 109695. [[CrossRef](#)]
18. Chen, Y.Y.; Hong, U.T.; Shih, H.C.; Yeh, J.W.; Duval, T. Electrochemical kinetics of the high entropy alloys in aqueous environments—A comparison with type 304 stainless steel. *Corros. Sci.* **2005**, *47*, 2679–2699. [[CrossRef](#)]
19. Chen, Y.Y.; Duval, T.; Hung, U.D.; Yeh, J.W.; Shih, H.C. Microstructure and electrochemical properties of high entropy alloys a comparison with type-304 stainless steel. *Corros. Sci.* **2005**, *47*, 2257–2279. [[CrossRef](#)]
20. Günen, A. Tribocorrosion behavior of boronized Co_{1.19}Cr_{1.86}Fe_{1.30}Mn_{1.39}Ni_{1.05}Al_{0.17}B_{0.04} high entropy alloy. *Surf Coat Tec.* **2021**, *421*, 127426. [[CrossRef](#)]
21. Karakas, M.S.; Günen, A.; Çarboga, C.; Karaca, Y.; Demir, M.; Altınay, Y.; Erdogan, A. Microstructure. Some mechanical properties and tribocorrosion wear behavior of boronized Al_{0.07}Co_{1.26}Cr_{1.80}Fe_{1.42}Mn_{1.35}Ni_{1.10} high entropy alloy. *J. Alloys Compd.* **2021**, *886*, 161222. [[CrossRef](#)]
22. Wang, W.; Sun, Q.; Wang, D.; Hou, J.; Qi, W.; Li, D.; Xie, L. Microstructure and Mechanical Properties of the ((CoCrFeNi)₉₅Nb₅)_{100-x}Mo_x High-Entropy Alloy Coating Fabricated under Different Laser Power. *Metals* **2021**, *11*, 1477. [[CrossRef](#)]
23. Lu, Y.; Gao, X.; Jiang, L.; Chen, Z.; Wang, T.; Jie, J.; Kang, H.; Zhang, Y.; Guo, S.; Ruan, H.; et al. Directly cast bulk eutectic and near-eutectic high entropy alloys with balanced strength and ductility in a wide temperature range. *Acta Mater.* **2017**, *124*, 143–150. [[CrossRef](#)]
24. Li, W.; Li, J.; Xu, Y. Investigation into the Corrosion Wear Resistance of CoCrFeNiAl_x Laser-Clad Coatings Mixed with the Substrate. *Metals* **2022**, *12*, 460. [[CrossRef](#)]
25. Jiang, H.; Jiang, L.; Qiao, D.; Lu, Y.; Wang, T.; Cao, Z.; Li, T. Effect of Niobium on Microstructure and Properties of the CoCrFeNb_xNi High Entropy Alloys. *J. Mater. Sci. Technol.* **2017**, *33*, 712–717. [[CrossRef](#)]
26. Wang, L.; Gao, Z.; Wu, M.; Weng, F.; Liu, T.; Zhan, X. Influence of Specific Energy on Microstructure and Properties of Laser Cladded FeCoCrNi High Entropy Alloy. *Metals* **2020**, *10*, 1464. [[CrossRef](#)]
27. Padamata, S.K.; Yasinskiy, A.; Yanov, V.; Saevarsdotir, G. Magnetron Sputtering High-Entropy Alloy Coatings: A Mini-Review. *Metals* **2022**, *12*, 319. [[CrossRef](#)]
28. Zhao, J.; Ma, A.; Ji, X.; Jiang, J.; Bao, Y. Slurry Erosion Behavior of Al_xCoCrFeNiTi_{0.5} High-Entropy Alloy Coatings Fabricated by Laser Cladding. *Metals* **2018**, *8*, 126. [[CrossRef](#)]
29. Löbel, M.; Lindner, T.; Kohrt, C.; Lampke, T. Processing of AlCoCrFeNiTi high entropy alloy by atmospheric plasma spraying. *IOP Conf. Ser. Mater. Sci. Eng.* **2017**, *181*, 12015. [[CrossRef](#)]

30. Li, J.; Huang, Y.; Meng, X.; Xie, Y. A Review on High Entropy Alloys Coatings: Fabrication Processes and Property Assessment. *Adv. Eng. Mater.* **2019**, *21*, 1900343. [[CrossRef](#)]
31. Shon, Y.; Joshi, S.S.; Katakam, S.; Rajamure, R.S.; Dahotr, N.B. Laser additive synthesis of high entropy alloy coating on aluminum: Corrosion behavior. *Mater. Lett.* **2015**, *142*, 122–125. [[CrossRef](#)]
32. Hua, N.B.; Wang, W.J.; Wang, Q.T.; Ye, Y.X.; Lin, S.H.; Zhang, L.; Guo, Q.H.; Brechtel, J.; Liaw, P.K. Mechanical, corrosion, and wear properties of biomedical Ti–Zr–Nb–Ta–Mo high entropy alloys. *J. Alloys Compd.* **2021**, *861*, 157997. [[CrossRef](#)]
33. Sun, Z.; Zhang, M.; Wang, G.; Yang, X.; Wang, S. Wear and corrosion resistance analysis of FeCoNiTiAl_x high-entropy alloy coatings prepared by laser cladding. *Coatings* **2021**, *11*, 155. [[CrossRef](#)]
34. Qiua, X. Microstructure and corrosion properties of Al₂CrFeCoxCuNiTi high entropy alloys prepared by additive manufacturing. *J. Alloys Compd.* **2021**, *887*, 161422. [[CrossRef](#)]
35. Wen, X.; Cui, X.; Jin, G.; Liu, Y.; Zhang, Y.; Fang, Y. In-situ synthesis of nano-lamellar Ni_{1.5}CrCoFe_{0.5}Mo_{0.1}Nb_x eutectic highentropy alloy coatings by laser cladding: Alloy design and microstructure evolution. *Surf. Coat. Technol.* **2021**, *405*, 126728. [[CrossRef](#)]
36. Wu, B.; Rao, C.; Dai, P. Effect of Silicon Content on the Microstructure and Wear Resistance of FeCoCr_{0.5}NiBSix High-entropy Alloy Coatings. *Surf. Technol.* **2015**, *44*, 85–91.
37. He, W.; Sun, R.; Niu, W.; Li, X.; Gu, M.; Zuo, R. Study on Microstructure and Corrosion Resistance of CoCrFeNiSix High-entropy Alloy Coating by Laser Cladding. *Surf. Technol.* **2021**, *50*, 343–348.
38. Yu, F.; Huang, C.; Du, C.; Li, J.; Dai, C.; Luo, H.; Liu, Z.; Li, X. Evolution in microstructure wear corrosion and tribocorrosion behavior of Mo-containing high-entropy alloy coatings fabricated by laser cladding. *Corros Sci.* **2021**, *191*, 109727.
39. Huang, B.; Zhang, C.; Cheng, H. Microstructure and Wear Resistance of FeCoCr_xNiB High-entropy Alloy coatings Prepared by Laser Cladding. *China Surf. Eng.* **2014**, *27*, 82–88.
40. Xu, Q.-L.; Liu, K.-C.; Wang, K.-Y.; Lou, L.Y.; Zhang, Y.; Li, C.-J.; Li, C.X. Al diffusion behavior of CuAl_xNiCrFe high-entropy alloys fabricated by high-speed laser cladding for TBC bond coats ScienceDirect. *Corros Sci.* **2021**, *192*, 109781. [[CrossRef](#)]
41. An, X.; Liu, Q. Effect of WC particles on the structure and properties of laser melting coated high entropy alloy SiFeCoCrTi coating. *Rare Met. Mater. Eng.* **2016**, *45*, 2424–2428.
42. Yan, G.; Zheng, M.; Ye, Z. In-situ Ti(C, N) reinforced AlCoCrFeNiSi-based high entropy alloy coating with functional gradient double-layer structure fabricated by laser cladding. *J. Alloys Compd.* **2021**, *886*, 161252. [[CrossRef](#)]
43. Wang, H.; Zhang, W.; Peng, Y.; Zhang, M.; Liu, Y. Microstructures and Wear Resistance of FeCoCrNi-Mo High Entropy Alloy/Diamond Composite Coatings by High Speed Laser Cladding. *Coatings* **2020**, *10*, 300. [[CrossRef](#)]
44. Guo, Y.; Liu, Q. MoFeCrTiWAlNb refractory high-entropy alloy coating fabricated by rectangular-spot laser cladding. *Intermetallics* **2018**, *102*, 78–87. [[CrossRef](#)]
45. Cong, N.; Yan, S.; Jia, L.; Huang, G. Characterization of Al_{0.5}FeCu_{0.7}NiCoCr high-entropy alloy coating on aluminum alloy by laser cladding. *Opt. Laser Technol.* **2018**, *105*, 257–263.
46. Shu, F.; Zhang, B.; Liu, T.; Sui, S.; Liu, Y.; He, P.; Liu, B.; Xu, B. Effects of laser power on microstructure and properties of laser clad CoCrBFeNiSi high-entropy alloy amorphous coatings. *Surf. Coat. Technol.* **2019**, *358*, 667–675. [[CrossRef](#)]
47. Chao, Q.; Guo, T.; Jarvis, T.; Wu, X.; Hodgson, P.; Fabijanic, D. Direct Laser Deposition Cladding of Al_xCoCrFeNi High Entropy Alloys on a High-temperature Stainless Steel. Surface and Coatings Technology. *Surf. Coat. Technol.* **2017**, *332*, 440–451. [[CrossRef](#)]
48. Zhao, R.; Yu, G.; He, X.; Li, H.; Li, S. Research on Laser Cladding Processing for 38MnV56 by PCA-TOPSIS Method. *Acta Armamentarii* **2019**, *40*, 2537–2544.
49. Liu, H.; Liu, J.; Li, X.; Chen, P.; Yang, H.; Hao, J. Effect of heat treatment on phase stability and wear behavior of laser clad AlCoCrFeNiTi 0.8 high-entropy alloy coatings. *Surf. Coat. Technol.* **2020**, *392*, 125758. [[CrossRef](#)]
50. Huang, C.; Zhang, Y.; Vilar, R.; Shen, J. Dry sliding wear behavior of laser clad TiVCrAlSi high entropy alloy coatings on Ti–6Al–4V substrate. *Mater. Des.* **2012**, *41*, 338–343. [[CrossRef](#)]
51. Li, M.; Zhang, Q.; Han, B.; Song, L.; Li, J.; Zhang, S. Effects of ultrasonic impact treatment on structures and properties of laser cladding Al_{0.5}CoCrFeMnNi high entropy alloy coatings. *Mater. Chem. Phys.* **2021**, *258*, 123850. [[CrossRef](#)]
52. Wen, X.; Cui, X.; Jin, G.; Zhang, X.; Zhang, Y.; Zhang, D.; Fang, Y. Design and characterization of FeCrCoAlMn_{0.5}Mo_{0.1} high-entropy alloy coating by ultrasonic assisted laser cladding. *J. Alloys Compd.* **2020**, *835*, 155449. [[CrossRef](#)]
53. Li, G.; Liu, J.; Chang, L. Preparation of CrFeNiSiAl_{0.5} High Entropy Alloy Coating by Doping Chromite Powder and Its Microstructure and Properties. *Surf. Eng.* **2021**, *50*, 271–276.
54. Chen, G.; Zhang, C.; Tang, Q.; Dai, P. Effect of Boron Addition on the Microstructure and Wear Resistance of FeCoCrNiB_x (x = 0.5, 0.75, 1.0, 1.25) High-Entropy alloy Coating Prepared by Laser Cladding. *Rare Met. Mater. Eng.* **2015**, *44*, 1418–1422.
55. Liu, H.; Gao, Q.; Man, J.; Li, X.; Yang, H.; He, J. Microstructure and Properties of CoCrFeMnNiTi_x High-entropy Alloy Coating by Laser Claddin. *Chin. J. Lasers* **2021**, *49*, 1–18.
56. Chen, L.; Wang, Y.; Hao, X. Lightweight refractory high entropy alloy coating by laser cladding on Ti–6Al–4V surface. *Vacuum* **2020**, *183*, 109823. [[CrossRef](#)]
57. Jiang, X.J.; Wang, S.Z.; Fu, H. A novel high-entropy alloy coating on Ti-6Al-4V substrate by laser cladding. *Mater. Lett.* **2022**, *308*, 131131. [[CrossRef](#)]
58. Xiang, K.; Chai, L.; Zhang, C.; Guan, H.; Wang, Y.; Ma, Y.; Sun, Q.; Li, Y. Investigation of microstructure and wear resistance of laser-clad CoCrNiTi and CrFeNiTi medium-entropy alloy coatings on Ti sheet—ScienceDirect. *Opt. Laser Technol.* **2022**, *145*, 107518. [[CrossRef](#)]

59. Zhao, P.; Li, J.; Zhang, Y.; Li, X.; Xia, M.M.; Yuan, B.G. Wear and high-temperature oxidation resistances of AlNbTaZrx high-entropy alloys coatings fabricated on Ti6Al4V by laser cladding. *J. Alloys Compd.* **2021**, *862*, 158405. [[CrossRef](#)]
60. Zhang, S.; Han, B.; Li, M.; Zhang, Q.; Hu, C.; Niu, S.; Li, Z.; Wang, Y. Investigation on solid particles erosion resistance of laser cladded CoCrFeNiTi high entropy alloy coating. *Intermetallics* **2021**, *131*, 107111. [[CrossRef](#)]